

Texture Evolution during the Processing of Electrical Steels with 0.5% Si and 1.25% Si

Marcos F. de CAMPOS, Fernando J. G. LANDGRAF,¹⁾ Ivan G. S. FALLEIROS,²⁾ Gabriela C. FRONZAGLIA³⁾ and Henrique KAHN³⁾

Programa de Pós-Graduação em Engenharia Metalúrgica, EEIMVR, Universidade Federal Fluminense, Av. dos Trabalhadores, 420 Vila Santa Cecília, 27255-125, Volta Redonda, RJ, Brazil. E-mail: mcampos@metal.eeimvr.uff.br

1) Instituto de Pesquisas Tecnológicas do Estado de São Paulo, Brazil. 2) Depto. de Engenharia Metalúrgica e de Materiais, Escola Politécnica, Universidade de São Paulo, Brazil. 3) Depto. de Engenharia de Minas, Escola Politécnica, Universidade de São Paulo, Brazil.

(Received on May 11, 2004; accepted in final form on July 21, 2004)

The development of the crystallographic texture in the processing of a 0.5% Si semi-processed steel sheet has been investigated. The results were also compared with those of a steel with 1.25% Si and 0.22% Al, to verify the effect of the chemical composition. The texture was examined after the following steps: i) hot band ii) 80–90% cold reduction iii) annealed iv) after skin pass v) after final annealing. The texture is very similar for both chemical compositions. The hot band presents an almost random texture. After 80–90% cold reduction, a typical rolling texture of steels is observed, containing the fibers $\langle 110 \rangle // \text{RD}$ and $\langle 111 \rangle // \text{ND}$. After annealing, the fiber $\langle 111 \rangle // \text{ND}$ is the most important component, but now with maximum at $\{111\}\langle 112 \rangle$. After skin pass and final annealing, the main components are the fiber $\{111\}\langle uvw \rangle$ and Goss $\{110\}[001]$. The results indicate that the Goss intensity tends to increase for smaller values of skin pass (where final grain size also increases). The change of Si content (from 0.5% up to 1.25% Si) and of Al (from ~0 upto 0.22%) did not produce significant variation about the texture components.

KEY WORDS: electrical steels; texture; recrystallization.

1. Introduction

The ideal texture for non-oriented electrical steels is $\{100\}\langle 0vw \rangle$. Nevertheless, there is no commercial (low-cost) method able to attain that texture. So, the usual procedure for texture optimization in non-oriented electrical steels is by avoiding grains with orientation such as $\{111\}$ or $\{211\}$, *i.e.* planes without easy magnetization direction parallel to the plane of the sheet, trying to replace them by grains like $\{100\}$ or $\{110\}$.

Electrical steel texture development has been investigated^{1–9)} and the effect of the hot band grain size has been the subject of several studies.^{6–8)} But, more specifically, the effect of silicon on the texture development of semi-processed electrical steels was not studied in depth. Among the reports on this subject are those of Kestens *et al.*¹⁾ that discussed the recrystallization texture in high Si steels and Hou,²⁾ which found more favorable recrystallization textures for steels with higher Si content. Few data is available about the effect of Si on deformation texture, and one of the rare studies is that of Sudo *et al.*,⁹⁾ often mentioned in reviews.^{10,11)}

The aim of this work is examining the texture in all steps of the processing of semi-processed electrical steels, and providing data about both, the deformation and recrystallization textures in Si steels.

In this study, we follow the change of crystallographic

texture of a 0.5% Si steel sheet during processing. The results are also compared with those of a 1.25% Si and 0.22% Al steel sheet, to acquire data about the effect of chemical composition. The texture data come from the steps: i) hot band, ii) after 80–90% cold reduction, iii) annealed, iv) after skin pass, v) after final annealing and recrystallization.

2. Experimental

Steel samples were processed in such way to reproduce typical conditions of industrial production. The A and B alloys permit us follow the evolution of texture during the processing of semi-processed electrical steels with different Si and Al content. The composition of the alloys are presented in **Table 1**.

A and B samples were submitted to the following processing:

Hot rolling to 2.7 mm: soaking temperature of 1150°C, finishing temperature 900°C, plus 5 h at 750°C, producing grain size of $18 \pm 2 \mu\text{m}$ (alloy A) and $16 \pm 2 \mu\text{m}$ (alloy B).

Table 1. Chemical composition and electrical resistivity of alloys A and B.

Alloy	%Si	%Al	%Mn	%P	%S	N (ppm)	ρ ($\mu\Omega\cdot\text{cm}$)
A	0.54	0.04	0.31	0.045	0.006	53	20.5
B	1.25	0.22	0.3	0.01	0.005	54	32

Table 2. Codes for the different samples of alloys A and B.

name	Step
HB	Hot band
CR	Cold rolled, ~80% reduction
N	After intermediary annealing under nitrogen
V	After intermediary annealing under vacuum
XX%	Skin-pass reduction
FA	Final Annealed

Those samples will be named A-HB and B-HB (where HB means “hot band”).

The same samples were, in a further step, cold rolled from ~2.7 mm down to ~0.53 mm of thickness, a 80% reduction. The cold rolled samples will receive the denomination A-CR and B-CR. These samples were submitted to two different types of intermediate annealing: one under nitrogen and other under vacuum.

There is slight difference concerning the different cycles:
Nitrogen:

slow heating holding at 680°C for 5 h, slow cooling

Vacuum:

heating at 1000°C/h, holding 720°C during 5 min,
cooling at 200°C/h

After these cycles, the measured grain size was (N: 14–15±2 μm) (V: 11–12±2 μm).

The samples after intermediate annealing will be called of A and B (followed by N or V, according to the kind of annealing).

After the intermediate annealing, A and B samples suffered skin-pass between 4 to 20% reduction. After all, they were recrystallized. Thus, the number XX%, refers to skin-pass, and FA means they were submitted to final annealing at 760°C for 2 h under a decarburizing atmosphere. The codes applied for the samples are given in **Table 2**.

The crystallographic texture was evaluated by means of ODFs calculated with harmonic method from X-ray pole figures¹²⁾ obtained in a Philips X-Pert XRD diffractometer equipped with texture goniometer.

3. Results and Discussion

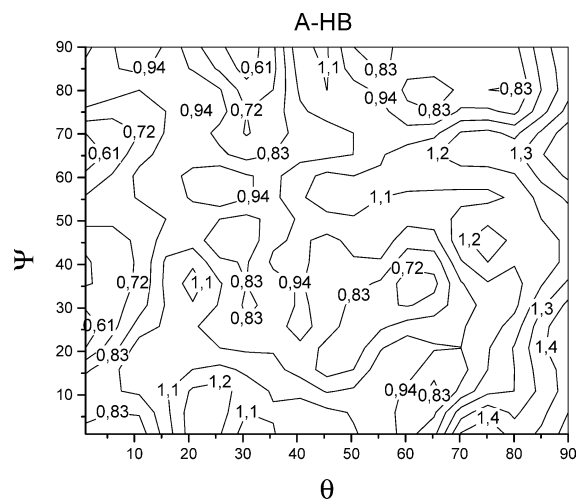
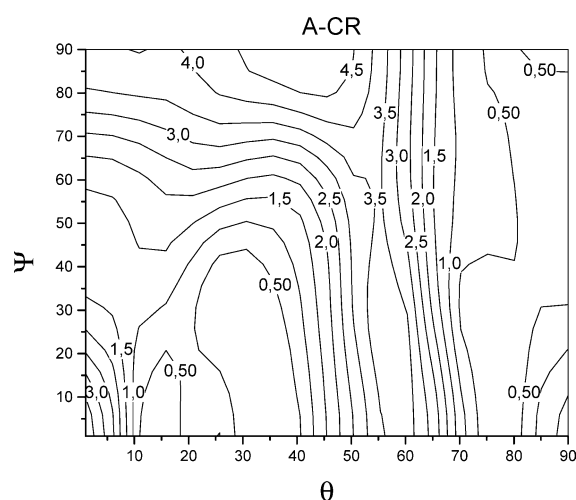
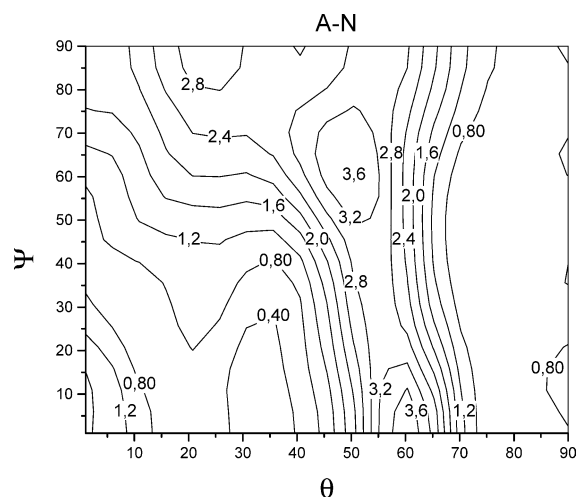
3.1. Texture Evolution during the Processing of a 0.5 % Si Electrical Steel (Alloy A)

In the sample A-HB (**Fig. 1**), we note a very random texture. The planes {110} are slightly more prominent, with Goss (110)[001] as the most important component in this weak texture.

We note in sample A-CR (**Fig. 2**) a typical rolling texture, often found in steels. The texture of sample A-CR has as main components the fibers <110>//RD (with maximum at (211)[0 $\bar{1}$ 1]) and <111>//ND (with maximum at {111}<110>).

In the sample A-N (**Fig. 3**) fiber <111>//ND is still present after recrystallization, but now with maximum at {111}<112>. Other important component is a fiber {100}<0vw> with maximum at {100}<011>. It is very important to note that several of recrystallization components tend to appear in a range with orientation difference between 15° to 35° when compared with the components in the parent situation (sample A-CR, Fig. 2).

For sample A-V (**Fig. 4**), an almost identical trend of sample A-N (Fig. 3) is followed, fiber <111>//ND.


Fig. 1. Sample A-HB. ODF, section $\Phi=45^\circ$. Roe Notation.

Fig. 2. Sample A-CR. ODF, section $\Phi=45^\circ$. Roe Notation.

Fig. 3. Sample A-N. ODF, section $\Phi=45^\circ$. Roe Notation.

Two samples A-V received different skin-passes, 4% and 17%. After final anneal, sample A-V 4% FA presented grain size of 360 μm, while the grain size was 48 μm in sample A-V 17% FA.

The grain size of sample A-V 4% FA is too large, thwarting the sampling due to the small number of grains

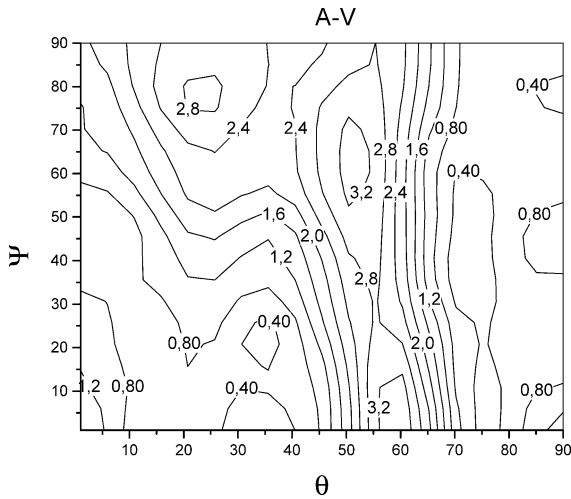


Fig. 4. Sample A-V. ODF, section $\Phi=45^\circ$. Roe Notation.

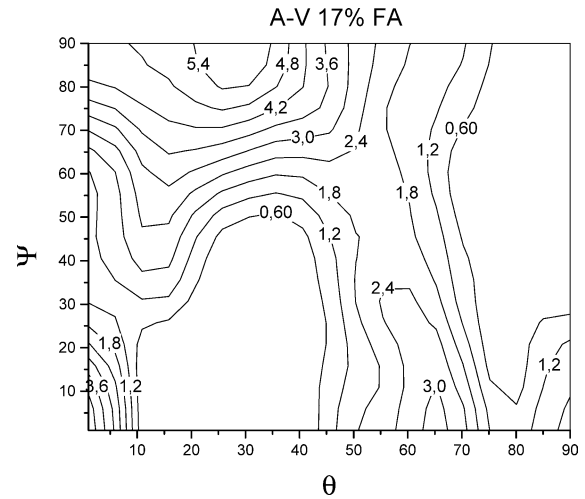


Fig. 6. Sample A-V 17% FA. ODF, section $\Phi=45^\circ$. Roe Notation.

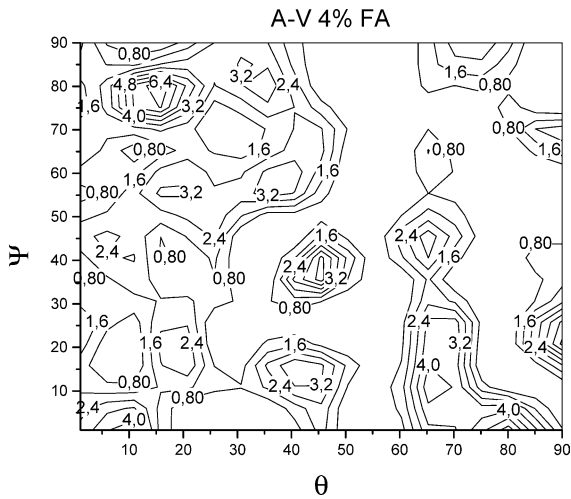


Fig. 5. Sample A-V 4% FA. ODF, section $\Phi=45^\circ$. Roe Notation.

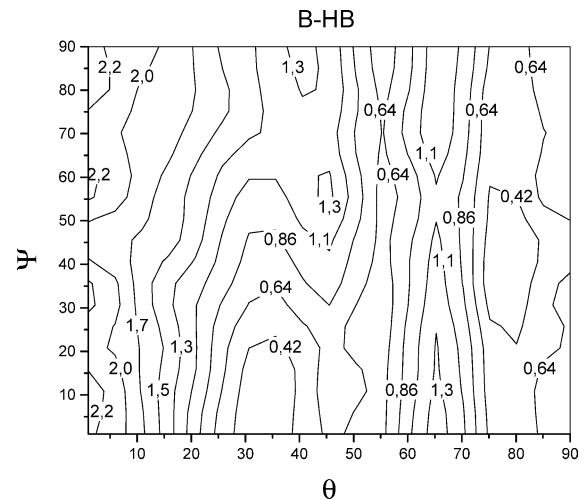


Fig. 7. Sample B-HB. ODF, section $\Phi=45^\circ$. Roe Notation.

measured to produce pole figures. Thus, this data may not be representative. The main components (Fig. 5) are near $\{100\}\langle 011\rangle$ and $\{110\}\langle 001\rangle$.

In the sample A-V 17% FA, we also note the tendency of “inversion” of the maximum of the fiber $\langle 111\rangle//ND$ (now with the maximum at $\{111\}\langle 110\rangle$) after recrystallization, see at sample A-N (compare Fig. 6 with Fig. 4). The fiber $\langle 110\rangle//RD$ is also present, with maximum at $\{211\}\langle 011\rangle$. Goss $(110)[001]$ has high intensity, but the component $\{100\}\langle 011\rangle$ is also very important. This texture is very similar to that of Fig. 2 (except the presence of Goss), showing that texture components may “reappear”, after the process of annealing + rolling + annealing (but now as a recrystallization texture).

3.2. Texture Evolution during the Processing of a 1.25% Si Electrical Steel (Alloy B)

The texture observed for the samples of alloy B, Figs. 7 up to 10 is quite similar to the textures of alloy A samples, presented in Figs. 1 to 4. The difference between the samples of A and B alloys are the Si and Al content (Table 1). Thus the obtained results allow us to infer that, in this case (*i.e.* for this specific experiment) the change of Si content almost did not affect the texture.

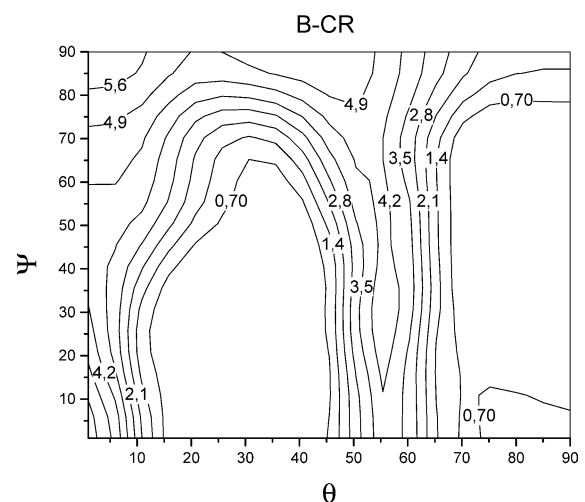


Fig. 8. Sample B-CR. ODF, section $\Phi=45^\circ$. Roe Notation.

For the sample B-HB (Fig. 7), we observe an almost random texture with a fibers $\{100\}\langle 0vw\rangle$ and $\langle 111\rangle//ND$ of weak intensity. The sample B-CR (Fig. 8) presents, again (as in Fig. 2), a typical rolling texture with the fibers $\langle 110\rangle//RD$ and $\langle 111\rangle//ND$, this last one with maximum at

Acknowledgements

MF de Campos thanks support from CAPES (Programa ProDoc) and FAPESP (Proc. 01/09122-4). All authors also thank FAPESP Proc. 99/10796-8).

REFERENCES

- 1) L. Kestens, J. J. Jonas, P. van Houtte and E. Aernoudt: *Metall. Trans. A*, **27A** (1996), 2347.
- 2) C.-K. Hou: *J. Magn. Magn. Mater.*, **162** (1996), 280.
- 3) J. Park, J. A. Szpunar and S. Cha: *Mater. Sci. Forum*, **408-412** (2002), 1263.
- 4) M. Shiozaki and Y. Kurosaki: *Textures Microstruct.*, **11** (1989), 159.
- 5) S. W. Cheong, E. J. Hilinski and A. D. Rollett: *Metall. Trans. A*, **34A** (2003), 1311.
- 6) H. Yashiki and A. Okamoto: *IEEE Trans. Mag.*, **23** (1987), 3086.
- 7) C.-K. Hou: *ISIJ Int.*, **36** (1996), 563.
- 8) M. F. de Campos, F. J. G. Landgraf, R. Takanohashi, F. C. Chagas, I. G. S. Falleiros, G. C. Fronzaglia and H. Kahn: *ISIJ Int.*, **44** (2004), 591.
- 9) M. Sudo, S. Hashimoto and I. Tsukatani: Proc. of 6th ICOTOM-Int. Conf. on Textures of Materials, ISIJ, Tokyo, (1981), 1076.
- 10) R. K. Ray, J. J. Jonas and R. E. Hook: *Int. Mater. Rev.*, **39** (1994), 129.
- 11) A. D. Rollet, S. I. Wright: *Texture and Anisotropy*, ed. by U. F. Kocks, C. N. Tomé and H.-R. Wenk, Cambridge University Press, Cambridge, (1998), 178.
- 12) R.-J. Roe: *J. Appl. Phys.*, **36** (1965), 2024.
- 13) F. J. G. Landgraf, R. Takanohashi, F. C. Chagas, M. F. de Campos and I. G. S. Falleiros: *J. Magn. Magn. Mater.*, **215-216** (2000), 92.
- 14) B. Hutchinson: *Philos. Trans. R. Soc. (London) A*, **357** (1999), 1471.
- 15) H. Inagaki: *Z. Metallkd.*, **78** (1987), 431.
- 16) H. Inagaki: *ISIJ Int.*, **34** (1994), 313.
- 17) M. Emura, M. F. de Campos, F. J. G. Landgraf and J. C. Teixeira: *J. Magn. Magn. Mater.*, **226-230** (2001), 1524.
- 18) M. F. de Campos, F. J. G. Landgraf and A. P. Tschiptschin: *J. Magn. Magn. Mater.*, **226-230** (2001), 1536.